Hindawi
Journal of Chemistry
Volume 2020, Article ID 7180347, 6 pages
https://doi.org/10.1155/2020/7180347

Research Article

Uniform Loading of Nickel Phosphide Nanoparticles in Hierarchical Carbonized Wood Channel for Efficient Electrocatalytic Hydrogen Evolution

Yuanjuan Bai, Yidan Zhang, Shihong Cheng, Yongfeng Luo, Kun Du, Jinbo Hu, and Xianjun Li

Hunan Province Key Laboratory of Materials Surface & Interface Science and Technology, College of Material Science and Engineering, Central South University of Forestry and Technology, Changsha 410004, China

Correspondence should be addressed to Xianjun Li; lxjmu@163.com

Received 4 December 2019; Accepted 10 March 2020; Published 10 April 2020

Guest Editor: Heng Jiang

The development of self-supporting high-efficiency catalysts is a major challenge for the efficient production of H_2 via water splitting. In this manuscript, a freestanding Ni_2P-$Ni_{12}P_5$/carbonized wood (CW) composite electrode was prepared by a simple hydrothermal method and high-temperature calcination using pine wood with uniform channel as support and a large number of hydroxyl groups as nucleation center. The morphology and structural characteristics indicated that the Ni_2P and $Ni_{12}P_5$ nanoparticles were uniformly distributed within the hierarchical porous structure of the CW. In acid media, the as-prepared Ni_2P-$Ni_{12}P_5$/CW exhibits an excellent catalytic activity with a low overpotential of 151 mV at 10 mA cm^{-2} and a reasonably good long-term stability.

1. Introduction

In order to realize the sustainable development of human society in the future, how to develop and utilize economic new clean energy has become a main research direction in energy area in the 21st century [1–4]. Direct electrochemical water splitting under room temperature and pressure by using electrocatalyst seems to represent one of the most sustainable and clean strategies for H_2 production. [5, 6]. The best well-known electrocatalytic catalyst for hydrogen evolution reaction (HER) is the precious metal platinum, which has high cost and limited reserves. Therefore, many researchers are paying great attention to the development of high-efficiency, cheap, and environmental-friendly HER catalysts.

Nickel phosphide, which is characterized by high activity, low cost, and earth-abundant, is considered to be one of the most potential alternative HER catalysts for Pt [7–10]. Nevertheless, there is still plenty of scope for improvement in preparation ways and performance. For example, in the traditional process of synthesizing nickel phosphide [11–13], PH_3 gas released through phosphatization reaction is a highly toxic substance, which will seriously pollute the environment. Moreover, the poor conductivity of metal phosphide makes electron transport difficult, which is usually improved by the addition of conductive carbon [14, 15] or metallic element [16, 17].

Wood is a cheap, biodegradable biomass material with well-aligned channels in the growth direction. After proper physical and chemical treatment, they can be derived into wood-based micro/nanomaterials with controllable structure and adjustable performance. These features make them promising materials for numerous applications including energy conversion, wastewater treatments, and microwave absorption [18–20]. At present, wood trunk in electrocatalysis area is still in its infancy, but very promising. A large number of studies have shown that the original channel structure can be maintained after the wood is carbonized at high temperature [21–23]. The resulting carbonized wood-

(CW-) based composites with a certain amount of graphitized carbon have good electrical conductivity, which is conducive to rapid electron transmission along the channel directions. Besides, they can be used directly as a self-standing electrode [24] and provides a strong combination between active substances and CW, leading to enhanced electron transport and stability over the long-term operation. However, it is not easy to load nanoparticles evenly in wood channels.

In this work, we selected the pine wood with uniform and regular channels as raw material and synthesized a Ni_2P-$Ni_{12}P_5$/CW heterostructure composite through alkali treatment, hydrothermal reaction, and high-temperature calcination successively. Different from the traditional nongreen preparation method of transition metal phosphides with sodium phosphite or PH_3 gas as the phosphorus source, the nontoxic NaH_2PO_4 was employed as the phosphorus source and the Ni-P-O precursor was loaded into the wood channel by a simple hydrothermal method. Then, the resulting Ni-P-O wood composites were calcined in an inert gas at a high temperature to obtain a self-standing, additive-free Ni_2P-$Ni_{12}P_5$/CW electrode. The reason for the uniform loading of the active nanoparticles in the wood channels is that the abundant hydroxyl groups in the wood tracheid wall can act as the nucleation center of precursors. Impressively, the as-developed self-standing Ni_2P-$Ni_{12}P_5$/CW electrode shows an excellent catalytic performance toward HER.

2. Materials and Methods

2.1. Materials. The pine wood was purchased from Chenzhou city, Hunan province, China. The reagents, including $NaH_2PO_4.2H_2O$, Ni $(NO_3)_2.6H_2O$, NH_4OH (≥28%), Na_2CO_3, H_2SO_4, NaOH, and Na_2SO_3, were purchased from Sinopharm Chemical Reagent Co, Ltd. Organic solvents, including ethylene glycol (AR) and absolute ethyl alcohol (AR), were obtained from Sigma Chemistry Co. Ltd. The deionized water was used to make up all mixed solutions and throughout the experiments.

2.2. Pretreatment of Pine Wood Slices. The pine wood slices were cut into chips with a size of 2*2*0.2 cm along the radial direction by a copping saw. The obtained wood slices were immersed in a mixed solution of NaOH (1 M) and Na_2SO_3 (1 M) with the volume ratio of 1 : 1 at 80°C for 24 h and then washed the slices with ethanol and deionized (DI) water in an ultrasonic cleaner for 20 min to remove soluble inorganic salts and other trace elements. Finally, the pine wood slices were dried at 80°C for 24 h in vacuum.

2.3. Preparation of Ni_2P-$Ni_{12}P_5$/CW Composite Electrode. The preparation process of the Ni_2P-$Ni_{12}P_5$/CW composite materials is shown schematically in Figure 1. Firstly, the Ni-P-O/wood composites were synthesized by a facile one-pot hydrothermal method. Typically, ethylene glycol (10 mL), NH_4OH (10 mL), an aqueous solution of Ni $(NO_3)_2$ (5 mL, 1 M), an aqueous solution of NaH_2PO_4 (7.5 mL, 1 M), and an aqueous solution of Na_2CO_3 (5 mL, 1 M) were mixed step by step under vigorous stirring. During this process, it takes two minutes to add the next solution. The reaction solution was rapidly stirred in ambient air for 5 min after the last substance is added. Secondly, the above solution was transferred into a 50 mL Teflon-lined autoclave, and a piece of wood substrate was immersed into the reaction solution, which was maintained at 150°C for 24 h in an electric oven to produce Ni-P-O/wood composite precursors. From the XRD pattern in Figure 2(a), we can see the Ni-P-O/wood composite was constituted of ammonium nickel phosphate and nickel phosphate. In this process, because of the abundance of hydroxyl group in the wood channels, it can be served as nucleation for Ni-P-O growth and finally make the Ni-P-O uniform and stable load on the wood channels. This nucleation mechanism was also mentioned in our previous work [25, 26]. After the equipment cooled down to room temperature naturally, the wood slice was fetched out and ultrasonically cleaned using distilled water and ethanol several times in order to remove the product on the surface. After that, the wood slice loaded with Ni-P-O was dried in vacuum at 80°C overnight. Finally, the Ni-P-O/wood was converted to Ni_2P-$Ni_{12}P_5$/CW after calcining in Ar atmosphere at 800°C for 200 min. The digital photograph of Ni-P-O/wood and Ni_2P-$Ni_{12}P_5$/CW composites in Figure 2(b) shows the volume of wood block materials has shrunk and the particle has successfully loaded onto the surface of the wood after calcination at high temperature.

2.4. Characterization. The morphologies and elemental analysis of the Ni_2P-$Ni_{12}P_5$/CW material were characterized using a scanning electron microscope (SEM, JSM-7800F, JEOL) equipped with an energy dispersive spectrometer (EDS). The crystal structures and phase characterization of them were measured by an X-ray diffractometer (X'Pert PRO, PANalytical) in the range of 5–90° (2θ). The specific surface area and pore distribution were examined using nitrogen adsorption and desorption isotherms on an automatic surface area and porosity analyzer (ASAP 2460, Micromeritics). The degree of graphitization of CW was conducted on a LabRAM HR Evolution (HORIBA Jobin Yvon SAS).

2.5. HER Experiments. All electrochemical tests were performed on CHI 760E chemical workstation (CH Instruments, Inc., Shanghai) using a typical three-electrode setup, with the graphite rod, saturated calomel electrode, and self-standing Ni_2P-$Ni_{12}P_5$/CW acting as the counter, reference, and working electrode, respectively. Linear sweep voltammetry (LSV) was performed on a solution of 0.5 M·H_2SO_4 with a scan rate of 5 mV·s^{-1}. All potentials measured were calibrated to RHE using the following equation: E (RHE) = E (SCE) + 0.059 × pH + 0.242. All experiments were carried out at room temperature (~25°C).

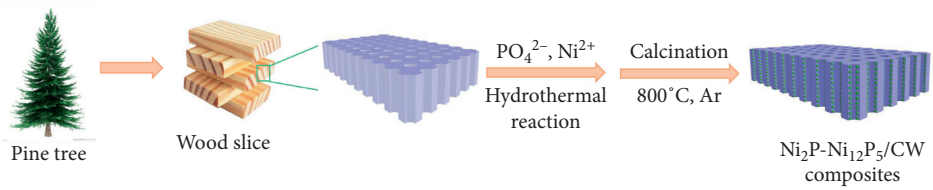

Figure 1: Schematic illustration of preparing the Ni_2P-$Ni_{12}P_5$/CW composite materials.

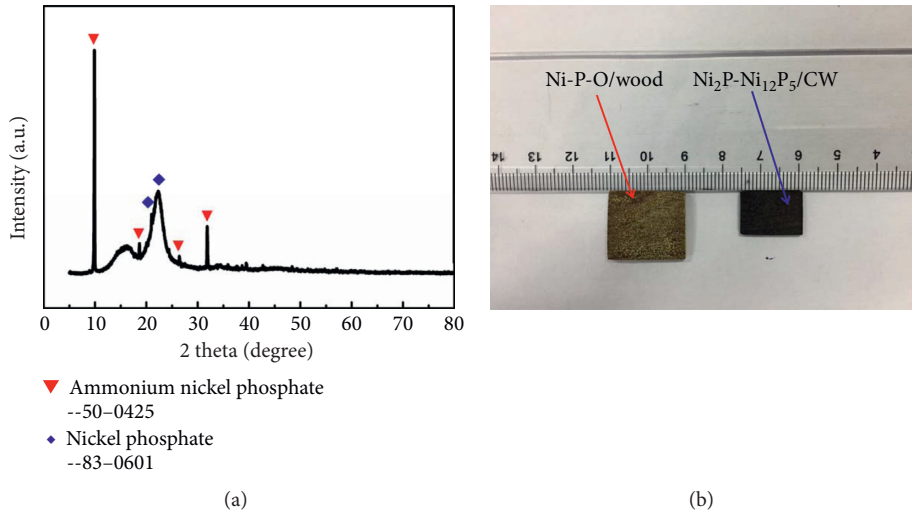

Figure 2: (a) Powder XRD pattern of the Ni-P-O precursors. (b) Digital photograph of Ni-P-O/wood and Ni_2P-$Ni_{12}P_5$/CW composites.

3. Results and Discussion

3.1. Phase, Morphology, Chemical Composition, and Structure Study of Ni_2P-$Ni_{12}P_5$/CW

3.1.1. XRD. At first, the crystal structure of the as-prepared products was characterized by the XRD patterns as shown in Figure 3. The samples show a set of obvious peaks at 40.7°, 44.6°, 47.4°, 54.2°, 55.0°, and 74.8°, corresponding to (111), (201), (210), (300), (211), and (400) of Ni_2P (JCPDS: 74–1385), respectively, suggesting the end-products containing hexagonal Ni_2P. Previous research studies have shown that Ni_2P is one of the best catalysts for HER. In addition, the samples also include another phase, which can be indexed to the tetragonal $Ni_{12}P_5$ (JCPDS: 22–1190). The diffraction peaks of both Ni_2P and $Ni_{12}P_5$ were sharp and intense, indicating their highly crystalline nature. Besides, we can see a broad peak at 23.4° and a weak peak at 26.4° in the pattern, which can be ascribed to the amorphous and graphitized carbon features of the CW block. These results indicate the obtained product is a composite material composed of Ni_2P, $Ni_{12}P_5$, and CW.

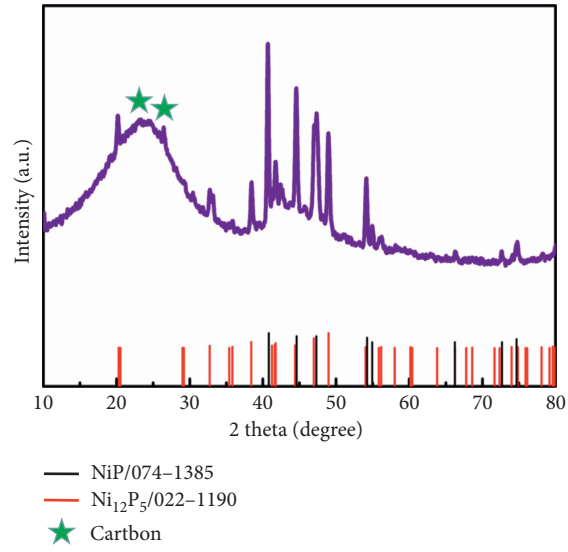

Figure 3: XRD patterns of Ni_2P-$Ni_{12}P_5$/CW composites.

3.1.2. SEM and EDS. Figure 4 shows some typical SEM images. From Figure 4(a), we can see clearly many straight channels along the growth direction of pine tree and the straight channels have different diameters and numerous small channels around the big channels. Figures 4(b) and 4(c) reveal that the Ni_2P-$Ni_{12}P_5$ nanoparticles are evenly dispersed in the CW's channels, and the size of nanoparticle is about 80 nm. Furthermore, the EDS data from Figure 5 demonstrate that the Ni_2P-$Ni_{12}P_5$/CW electrode mainly consists of Ni, P, and C elements. The trace amount of O element may be due to the material's exposure to the air. And the corresponding quantitative analysis of elements shows the atom ration of P/Ni = 1/3. After calculation, the molar ratio of Ni_2P to $Ni_{12}P_5$ is about 1/7.

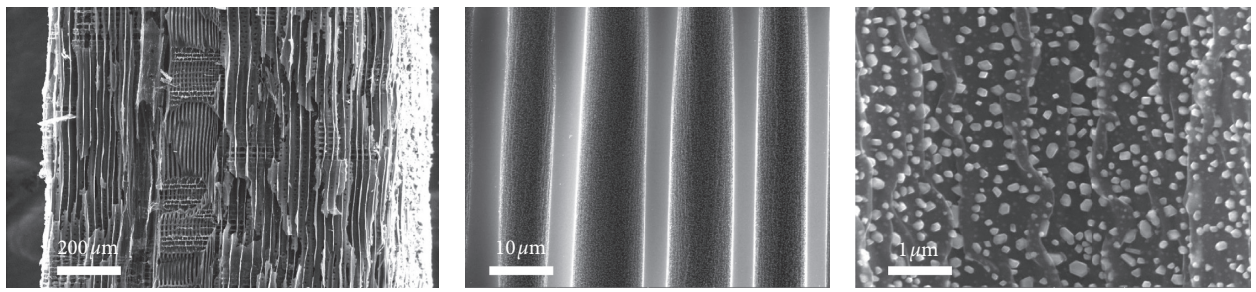

(a) (b) (c)

Figure 4: SEM images of Ni_2P-$Ni_{12}P_5$/CW at different magnifications.

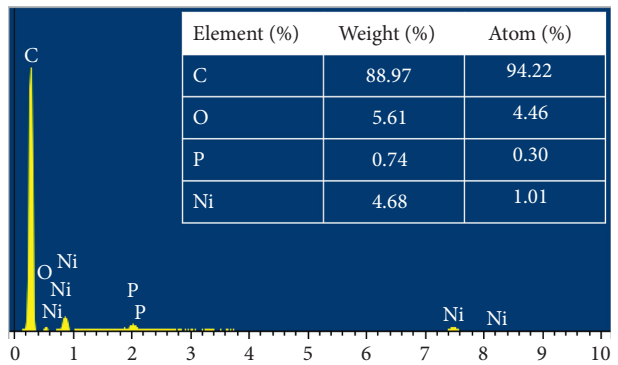

Element (%)	Weight (%)	Atom (%)
C	88.97	94.22
O	5.61	4.46
P	0.74	0.30
Ni	4.68	1.01

Figure 5: EDS spectra and element content analysis table of Ni_2P-$Ni_{12}P_5$/CW.

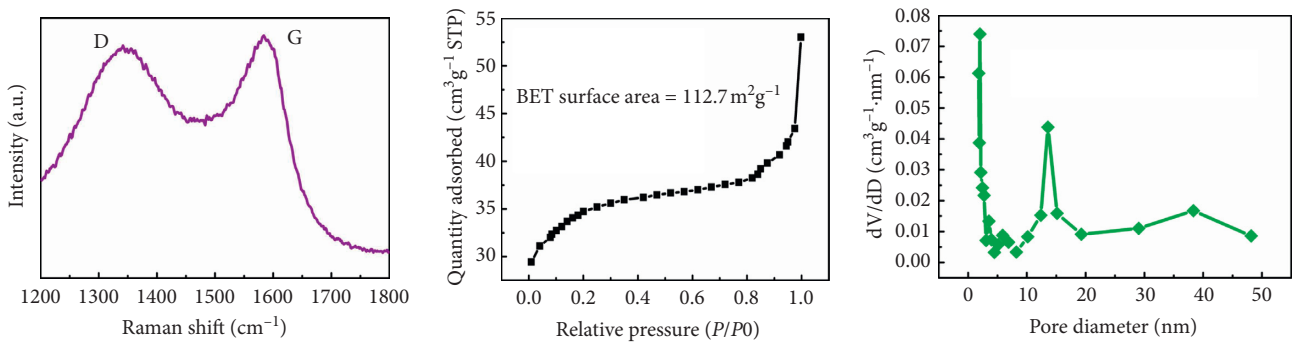

(a) (b) (c)

Figure 6: (a) Raman spectrum and (b, c) nitrogen adsorption-desorption isotherm of the prepared Ni_2P-$Ni_{12}P_5$/CW.

3.1.3. Raman Spectrum and Surface Area Study of Ni_2P-$Ni_{12}P_5$/CW. The Raman spectroscopy of the CW slice loading Ni_2P-$Ni_{12}P_5$ nanoparticles is presented in Figure 6(a). In the spectra, there are two characteristic bands: *D* band at around 1340 cm^{-1} and *G* band at about 1590 cm^{-1}, respectively, match well with amorphous and graphitized carbons. In theory, when the temperature of calcination reaches 800°C, some of the carbon in CW slice will be converted to graphitized carbon. As expected, the I_G/I_D ratio is about 1.05, which suggests good crystallization of the Ni_2P-$Ni_{12}P_5$/CW obtained after 800°C annealing. Nitrogen absorption/desorption analysis was applied to investigate the Brunauer–Emmett–Teller (BET) surface area and pore diameter of the Ni_2P-$Ni_{12}P_5$/CW samples. From Figure 6(b), we can see the BET surface area of the Ni_2P-$Ni_{12}P_5$/CW is about 112.7 $m^2 \cdot g^{-1}$. And this material has hierarchical pore structure, as shown in Figure 6(c).

3.2. Electrochemical Performance Study of Ni_2P-$Ni_{12}P_5$/CW. The HER catalytic activity of the integrated Ni_2P-$Ni_{12}P_5$/CW electrode is evaluated in 0.5 M·H_2SO_4 solution using a three-electrode cell. And using the acid corrosion method, the load mass of the active substances of the Ni_2P-$Ni_{12}P_5$/CW electrode could be calculated to be about 0.36 mg·cm^{-2}. Figure 7(a) displays the polarization curves of the Ni_2P-

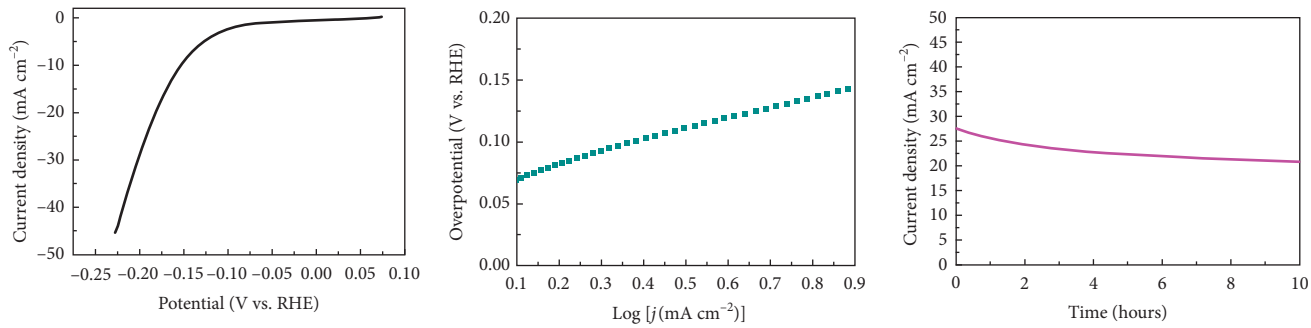

Figure 7: (a) Polarization curves and (b) Tafel plots calculated from polarization curves of the Ni_2P-$Ni_{12}P_5$/CW electrode in 0.5 M·H_2SO_4 at room temperature with a scan rate of 5 mV·s^{-1}. (c) Chronoamperometric profile of the electrode measured at −200 mV in 0.5 M·H_2SO_4.

$Ni_{12}P_5$/CW electrode. As expected, the Ni_2P-$Ni_{12}P_5$/CW electrode exhibits a good HER activity and achieved a current density of 10 mA·cm^{-2} at a low overpotential of 151 mV. Further insight into the catalytic activity of Ni_2P-$Ni_{12}P_5$/CW is obtained by extracting the slopes from the Tafel plots in Figure 7(b). The calculated value of Tafel slopes is about 79 mV dec^{-1}, which suggests that HER on Ni_2P-$Ni_{12}P_5$/CW occurs via a Volmer–Heyrovsky mechanism. In addition, the Ni_2P-$Ni_{12}P_5$/CW electrode also exhibits strong durability in strong acid media (Figure 7(c)). Based on the above discussion and experimental results, the reasons for the superior properties of Ni_2P-$Ni_{12}P_5$/CW can be ascribed to the following points. Firstly, abundant channels in the CW provide a large specific surface area, facilitating electrolyte infiltration. Secondly, the graphitized carbon of the Ni_2P-$Ni_{12}P_5$/CW has excellent electrical conductivity, which is conducive to rapid electron transport. Thirdly, this self-supporting electrode of Ni_2P-$Ni_{12}P_5$/CW allows electrons to move quickly between the electrode and the active material.

4. Conclusions

In this work, we chose a cheap biomass material pine wood as the raw material and introduced Ni-P-O precursors by a hydrothermal method using a large number of hydroxyl groups in the wood channel as the nucleation center. After a high-temperature calcination process, a self-supporting Ni_2P-$Ni_{12}P_5$/CW electrode with Ni_2P-$Ni_{12}P_5$ nanoparticles evenly dispersed in the CW channels was obtained. With the highly porous feature, large surface area, good electrical conductivity, extended electronic structure, and preeminent structural stabilization of CW, the Ni_2P-$Ni_{12}P_5$/CW electrode exhibits excellent HER activity and stability.

Data Availability

The data used to support the findings of this study are included within the article.

Conflicts of Interest

The authors declare that they have no conflicts of interest.

Acknowledgments

This research was supported by the National Natural Science Foundation of China (21908251), the Hunan high-level talent gathering project-innovative talents (no. 2019RS1061), and the introduction of Talent Research Startup Foundation of Central South University of Forestry and Technology (Grant no. 2017YJ003).

References

[1] U.S. Energy Information Administration, *International Energy Outlook*, U.S. Energy Information Administration, Washington, D.C., USA, 2016.

[2] British Petroleum, "Statistical review of world energy," British Petroleum, London, UK, 2017.

[3] B. Dunn, H. Kamath, and J.-M. Tarascon, "Electrical energy storage for the grid: a battery of choices," *Science*, vol. 334, no. 6058, pp. 928–935, 2011.

[4] W. Li, J. Liu, and D. Zhao, "Mesoporous materials for energy conversion and storage devices," *Nature Reviews Materials*, vol. 1, p. 16023, 2016.

[5] L. Rößner and M. Armbrüster, "Electrochemical energy conversion on intermetallic compounds: a review," *ACS Catalysis*, vol. 9, no. 3, pp. 2018–2062, 2019.

[6] D. A. Henckel, M. HenckelOlivia, O. M. Lenz, K. M. Krishnan, and B. M. Cossairt, "Improved HER catalysis through facile, aqueous electrochemical activation of nanoscale WSe2," *Nano Letters*, vol. 18, no. 4, pp. 2329–2335, 2018.

[7] C. Cossairt, R. Zhang, and W. Lu, "Energy-saving electrolytic hydrogen generation: Ni2P nanoarray as a high-performance non-noble-metal electrocatalyst," *Angewandte Chemie*, vol. 129, no. 3, pp. 860–864, 2017.

[8] J. Sun, Y. Chen, Z. Ren et al., "Self-supported NiS nanoparticle-coupled Ni_2P nanoflake array architecture: an advanced catalyst for electrochemical hydrogen evolution," *ChemElectroChem*, vol. 4, pp. 1–9, 2017.

[9] H. Wen, L.-Y. Gan, H.-B. Dai et al., "In situ grown Ni phosphide nanowire array on Ni foam as a high-performance catalyst for hydrazine electrooxidation," *Applied Catalysis B: Environmental*, vol. 241, pp. 292–298, 2019.

[10] R. Zhang, P. A. Russo, M Feist, P. Amsalem, N. Koch, and N. Pinna, "Synthesis of nickel phosphide electrocatalysts from hybrid metal phosphonates," *ACS Applied Materials & Interfaces*, vol. 9, no. 16, pp. 14013–14022, 2017.

[11] L.-A. Stern, L. Feng, F. Song, and X. Hu, "Ni2P as a Janus catalyst for water splitting: the oxygen evolution activity of Ni2P nanoparticles," *Energy & Environmental Science*, vol. 8, no. 8, pp. 2347–2351, 2015.

[12] A. Dutta, A. K. Samantara, S. K. Dutta, B. K. Jena, and N. Pradhan, "Surface-oxidized dicobalt phosphide nanoneedles as a nonprecious, durable, and efficient OER catalyst," *ACS Energy Letters*, vol. 1, no. 1, pp. 169–174, 2016.

[13] J. Chang, L. Liang, C. Li et al., "Ultrathin cobalt phosphide nanosheets as efficient bifunctional catalysts for a water electrolysis cell and the origin for cell performance degradation," *Green Chemistry*, vol. 18, no. 8, pp. 2287–2295, 2016.

[14] Y. Li, P. Cai, S. Ci, and Z. Wen, "Strongly coupled 3D nanohybrids with Ni2 P/carbon nanosheets as pH-universal hydrogen evolution reaction electrocatalysts," *ChemElectroChem*, vol. 4, no. 2, pp. 340–344, 2017.

[15] J. Chang, Y. Xiao, M. Xiao, J. Ge, C. Liu, and W. Xing, "Surface oxidized cobalt-phosphide nanorods as an advanced oxygen evolution catalyst in alkaline solution," *ACS Catalysis*, vol. 5, no. 11, pp. 6874–6878, 2015.

[16] Y. Lian, H. Sun, X. Wang et al., "Carved nanoframes of cobalt-iron bimetal phosphide as a bifunctional electrocatalyst for efficient overall water splitting," *Chemical Science*, vol. 10, no. 2, pp. 464–474, 2019.

[17] Q. Sun, M. Zhou, Y. Shen et al., "Hierarchical nanoporous Ni (Cu) alloy anchored on amorphous NiFeP as efficient bifunctional electrocatalysts for hydrogen evolution and hydrazine oxidation," *Journal of Catalysis*, vol. 373, pp. 180–189, 2019.

[18] Y. Wang, G. Sun, J. Dai et al., "A high-performance, low-tortuosity wood-carbon monolith reactor," *Advanced Materials*, vol. 29, no. 2, p. 1604257, 2017.

[19] L. A. Berglund and I. Burgert, "Bioinspired wood nanotechnology for functional materials," *Advanced Materials*, vol. 30, no. 19, p. 1704285, 2018.

[20] J. Song, C. Chen, S. Zhu et al., "Processing bulk natural wood into a high-performance structural material," *Nature*, vol. 554, no. 7691, pp. 224–228, 2018.

[21] Y. Li, M. Cheng, E. Jungstedt, B. Xu, L. Sun, and L. Berglund, "Optically transparent wood substrate for perovskite solar cells," *ACS Sustainable Chemistry & Engineering*, vol. 7, no. 6, pp. 6061–6067, 2019.

[22] S. Zhang, C. Wu, W. Wu et al., "High performance flexible supercapacitors based on porous wood carbon slices derived from Chinese fir wood scraps," *Journal of Power Sources*, vol. 424, pp. 1–7, 2019.

[23] Q. W. Jiang, G. R. Li, F. Wang, and X. P. Gao, "Highly ordered mesoporous carbon arrays from natural wood materials as counter electrode for dye-sensitized solar cells," *Electrochemistry Communications*, vol. 12, no. 7, pp. 924–927, 2010.

[24] H. S. Yaddanapudi, K. Tian, S. Teng, and A. Tiwari, "Facile preparation of nickel/carbonized wood nanocomposite for environmentally friendly supercapacitor electrodes," *Scientific Reports*, vol. 6, p. 33659, 2016.

[25] Y. Bai, H. Zhang, L. Fang, L. Liu, H. Qiu, and Y. Wang, "Novel peapod array of Ni2P@graphitized carbon fiber composites growing on Ti substrate: a superior material for Li-ion batteries and the hydrogen evolution reaction," *Journal of Materials Chemistry A*, vol. 3, no. 10, pp. 5434–5441, 2015.

[26] Y. Bai, L. Fang, H. Xu, X. Gu, H. Zhang, and Y. Wang, "Strengthened synergistic effect of metallic MxPy (M=Co, Ni, and Cu) and carbon layer via peapod-like architecture for both hydrogen and oxygen evolution reactions," *Small*, vol. 13, no. 16, p. 1603718, 2017.